Pergamon

Int. J. Heat Mass Transfer. Vol. 40, No. 14, pp. 3293–3304, 1997

Printed in Great Britain
0017–9310/97 $17.00+0.00

PII: S0017–9310(96)00381–X

Laminar forced convection in the entrance region of helical pipes

C. X. LIN, P. ZHANG and M. A. EBADIAN†

Hemispheric Center for Environmental Technology, Florida International University, Miami, FL 33199, U.S.A.

(*Received* 6 *August* 1996 *and in final form* 5 *November* 1996)

Abstract—In the present study, three-dimensional laminar forced flow and heat transfer in the entrance region of helical pipes have been investigated using a fully elliptic numerical method. Laminar flow and heat transfer were assumed to develop from the inlet to the outlet simultaneously. The governing equations were solved by means of a control-volume finite element method. The results presented in this paper cover a Reynolds number range of 250–2000, a pitch range of 0.0–0.6, and a curvature ratio range of 0.025–0.20. The present elliptic numerical results are compared with previous experimental data and parabolic numerical data. The developments of temperature field, main and secondary velocity fields, local and average friction factors, and local and average Nusselt numbers are given and discussed. It has been found that both the friction factor and Nusselt number are oscillatory in the entrance region of helical pipes. The pitch and Reynolds number exert different effects on the developments of the friction factor and Nusselt number than the curvature ratio. © 1997 Elsevier Science Ltd.

INTRODUCTION

Laminar forced flow and heat transfer in helical pipes with a constant circular cross section have wide applications in heat exchangers, piping systems, storage tanks, chemical reactors, and many other engineering systems [1, 2]. One of the principal features of the physical problem is the occurrence of a secondary flow in planes normal to the main flow. When affected by finite-pitch-induced torsion, this secondary flow dramatically increases the difficulty of theoretical analysis, and causes the heat and momentum transfer in helical pipes to be substantially different from that in straight pipes, as well as that in ordinary curved pipes. In contrast to the numerous studies on fully developed laminar flow and heat transfer in helical pipes, the available results on developing flow and heat transfer in the entrance region of helical pipes are relatively sparse, and the physics of the latter is not well understood.

Most of the previous studies on the developing laminar flow and heat transfer in helical pipes have been conducted for the case of a torus, i.e. a helical pipe of zero pitch. Experimental measurements of the developing fluid flow and heat transfer include those presented by Dravid *et al.* [3], Balejova *et al.* [4], Janssen and Hoogendoorn [5], Kalb and Seader [6], and Austen and Soliman [7]. Numerical computations of the developing fluid flow and heat transfer were reported by Patankar *et al.* [8], Tarbell and Samuels [9], Akiyama and Cheng [10], Soh and Berger [11], Padmanabhan [12], Acharya *et al.* [13], and Sillekens [14]. For the case of helical pipes with finite pitch, Liu and Masliyah [15] applied a finite difference method to investigate the developing laminar flow and heat transfer. The governing equation is fully parabolized in the axial direction. The developments of the Nusselt number at different Prandtl numbers and inlet conditions were reported, but the effects of curvature ratio, pitch, and Reynolds number on the development of the fluid flow and heat transfer were not examined separately. Moreover, as the developing flow inside the helical pipes was fully three-dimensional, the parabolic computation could lead to results of low accuracy or reality.

The purpose of this paper is to perform a fully elliptic numerical computation to study laminar developing flow and heat transfer in helical pipes with finite pitch. A control-volume finite element method (CVFEM) of second-order accuracy is used to solve the governing equations for the developing fluid flow and heat transfer. The effects of pitch, curvature ratio, and Reynolds number on the developments of friction factors and Nusselt numbers are presented and highlighted.

MATHEMATICAL FORMULATION

The geometry considered and the system of coordinates are depicted in Fig. 1. The circular pipe studied has a diameter of $2a$ and is coiled at a radius of R_c, while the distance between two turns (the pitch) is represented by H. In Fig. 1, **R** is the global coordinate vector, and **N** and **B** are the normal and binormal vectors, respectively, on the center line of the helical pipe. The orthogonal helical coordinate system (s, r, θ)

†Author to whom correspondence should be addressed.

NOMENCLATURE

a radius of the helical pipe [m]
A area [m^2]
C specific heat [kJ (kg K)$^{-1}$]
d_h hydraulic diameter of the helical pipe ($2a$) [m]
f_{fd} fully developed average friction factor
f_m circumferential average friction factor on one cross-section $\left(\frac{1}{2\pi}\int_0^{2\pi} f_\theta \, d\theta\right)$
f_θ local friction factor on the circumference of a pipe ($\tau_w/(0.5\rho u_0^2)$)
H pitch [m]
n coordinate direction perpendicular to a surface
Nu_{fd} fully developed average Nusselt number
Nu_m circumferential average Nusselt number on a cross section $\left(\frac{1}{2\pi}\int_0^{2\pi} Nu_\theta \, d\theta\right)$
Nu_θ local Nusselt number on the circumference of a pipe $[(q_w d_h/\Gamma_l)/(T_w - T_b)]$
p pressure [N m^{-2}]
Pr Prandtl number
q_w wall heat flux [W m^{-2}]
r radial coordinate [m]
R_c radius of the coil [m]
Re Reynolds number ($\rho u_0 d_h/\mu$)
s axial coordinate [m]
T temperature [K]
T_b fluid bulk temperature on one cross section $\left(\frac{1}{u_s A}\int_0^A u_s T \, dA\right)$ [K]
u_0 inlet velocity [m s^{-1}]
u_i velocity component in i-direction ($i = 1, 2, 3$) [m s^{-1}]
u_r radial velocity component [m s^{-1}]
u_θ velocity component in azimuthal direction [m s^{-1}]
U_s nondimensional axial velocity (u_s/u_b)
U_{2nd} nondimensional secondary velocity $[(u_r+u_\theta)^{1/2}/u_0]$
x_i master Cartesian coordinate in i-direction ($i = 1, 2, 3$) [m].

Greek symbols

α angle [°]
Γ thermal conductivity [W (m K)$^{-1}$]
δ curvature ratio (a/R_c)
δ_{ij} Dirac delta function
η, ζ orthogonal rectangular coordinate [m]
θ orthogonal azimuthal coordinate [°]
Θ nondimensional temperature $[(T-T_w)/(T_b-T_w)]$
λ nondimensional pitch $[H/(2\pi R_c)]$
μ viscosity [kg (m s)$^{-1}$]
ρ density of fluid [kg m^{-3}]
τ_w wall shear stress [N m^{-2}]
φ axial angle [°]
ϕ any variable.

Subscripts

0 inlet conditions
2nd secondary flow
fd fully developed condition
i, j, k general spatial indices (= 1, 2, 3)
r, θ, s radial, azimuthal and axial directions, respectively
w wall condition.

or (s, η, ζ) relative to the master Cartesian coordinate system (x_1, x_2, x_3) is similar to that used by Liu and Masliyah [15] and Germano [16]. The orthogonality of the helical coordinate system is achieved by rotating the bases formed by the Frenet frame **B** and **N** around the s-axis with

$$\theta = \alpha + \frac{H}{2\pi} s b^2 + \theta_0 \tag{1}$$

where θ_0 = constant, and $b = [R_c^2 + (H/2\pi)^2]^{-1/2}$. A given point in the helical pipe can be mapped to the master Cartesian system through

$$\mathbf{X} = \mathbf{R} + r\cos\alpha\mathbf{N} + r\sin\alpha\mathbf{B} \tag{2}$$

$$\mathbf{R} = \left(R_c\cos\varphi, R_c\sin\varphi, \frac{H}{2\pi}\varphi\right) \tag{3}$$

$$\mathbf{N} = (-\cos\varphi, -\sin\varphi, 0) \tag{4}$$

$$\mathbf{B} = \left(\frac{H}{2\pi} b\sin\varphi, -\frac{H}{2\pi} b\cos\varphi, bR_c\right). \tag{5}$$

The transformation metrics employed to set the helical coordinate system to be orthogonal can be found in the studies by Liu and Masliyah [15] and Germano [16]. The orthogonal system (s, r, θ) or (s, η, ζ), and the nonorthogonal system (s, r, α), share the same cross section.

At the inlet ($\varphi = 0°$), fluid at temperature T_0 enters into the helical pipe at a speed of u_0. The wall of the pipe is heated under constant temperature T_w. Laminar flow and heat transfer develop simultaneously downstream in the helical pipe. The flow is assumed to be steady and incompressible. The fully

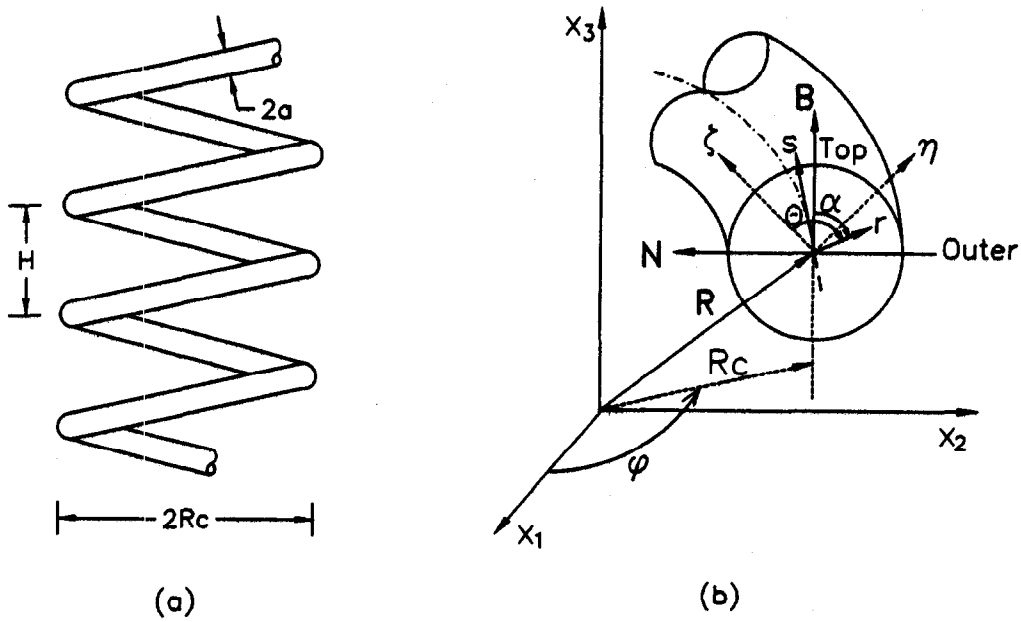

Fig. 1. Geometry and system of coordinates: (a) helical pipe; (b) helical coordinate system.

elliptic differential equations governing laminar flow in helical pipes can be written in tensor form as:

Mass:

$$\frac{\partial u_i}{\partial x_i} = 0 \tag{6}$$

Momentum:

$$\frac{\partial}{\partial x_j}\left[\mu\left(\frac{\partial u_i}{\partial x_j}+\frac{\partial u_j}{\partial x_i}\right)\rho u_j u_i - \delta_{ij}p\right] = 0 \tag{7}$$

Energy:

$$\frac{\partial}{\partial x_j}\left(\Gamma\frac{\partial T}{\partial x_j} - \rho u_j C T\right) + \mu\Phi_v = 0 \tag{8}$$

where

$$\Phi_v = \frac{\partial u_i}{\partial x_j}\left(\frac{\partial u_i}{\partial x_j}+\frac{\partial u_j}{\partial x_i}\right). \tag{9}$$

A nonslip boundary condition was imposed on the wall of the helical pipe. At the inlet, uniform profiles for all the dependent variables are employed for simplicity as follows:

$$u_s = u_0 \quad u_r = 0 \quad u_\theta = 0 \quad T = T_0 \tag{10}$$

where u_s, u_r and u_θ are the axial, radial and azimuthal velocities, respectively.

At the outlet, the diffusion flux for all variables in the exit direction are set to zero:

$$\frac{\partial}{\partial n}(u_s, u_r, u_\theta, T) = 0. \tag{11}$$

Here, n is used to represent the normal coordinate direction perpendicular to the outlet plane. The selection of the outlet plane location is based on the entry length data on curved pipes given by Austin and Seader [17] to ensure that fully developed flow results can be obtained on the outlet plane.

To represent the results, the following nondimensional variables and parameters are defined:

$$Re = \frac{\rho u_0 d_h}{\mu} \quad \delta = \frac{a}{R_c} \quad \lambda = \frac{H}{2\pi R_c}$$

$$T_b = \frac{1}{u_s A}\int_0^A u_s T\,dA \quad \Theta = \frac{T-T_w}{T_b - T_w}$$

$$U_s = \frac{u_s}{u_0} \quad U_{2nd} = \frac{(u_r^2+u_\theta^2)^{1/2}}{u_0}$$

$$f_\theta = \frac{\tau_w}{\frac{1}{2}\rho u_0^2} \quad f_m = \frac{1}{2\pi}\int_0^{2\pi} f_\theta\,d\theta$$

$$Nu_\theta = \frac{q_w d_h}{\Gamma(T_w - T_b)} \quad Nu_m = \frac{1}{2\pi}\int_0^{2\pi} Nu_\theta\,d\theta \tag{12}$$

where δ denotes the curvature ratio, λ the nondimensional pitch, d_h the hydraulic diameter ($2a$), f_θ and Nu_θ the local friction factor and Nusselt number along the circumference of the pipe, respectively, and f_m and Nu_m the circumferential average friction factor and Nusselt number on one cross section of the pipe, respectively. The friction factors and Nusselt numbers are defined using the wall shear stress, τ_w, and heat flux, q_w, respectively. The wall shear stress, τ_w, is computed based on the normal velocity gradient at the wall, and the heat flux, q_w is computed using Fourier's law applied at the wall. The term Θ represents nondimensional temperature, while U_s and U_{2nd} denote nondimensional axial velocity and secondary velocity on one cross section, respectively.

NUMERICAL COMPUTATION

The governing equations have been solved in the Cartesian master coordinate system with a CVFEM similar to that introduced by Baliga and Patankar [18]. The FLUENT/UNS code [19] has been used as the numerical solver for the present three-dimensional problem. As the CVFEM combines the best aspects of the control-volume finite difference method (CVFDM) and the finite element method (FEM), it provides the mesh flexibility of the FEM without sacrificing the benefits of the CVFDM, which are robustness and economy.

An unstructured (block-structured) nonuniform grid system was used to discrete the governing equations. Figure 2 depicts the unstructured grid used for the three-dimensional computation. Five blocks were applied to form the entire helical pipe, with the central square block occupying 12.4% of the area on each cross section. The relative position of the five blocks to the circumference and center line of the helical pipe was fixed on a certain plane, and all the subsurfaces used to hold the blocks were created with a curve-driven-surface technique [20].

The convection term in the governing equations was modeled with the bounded secondary-order upwind scheme, which uses the upwind value and gradient to compute the value at the control volume face. The diffusion term was computed using multilinear interpolating polynomials, $N_i(X, Y, Z)$ (also referred to as shape function in the FEM). The final discreted algebraic equation for variable ϕ at each node is a set of nominally linear equations that can be written as

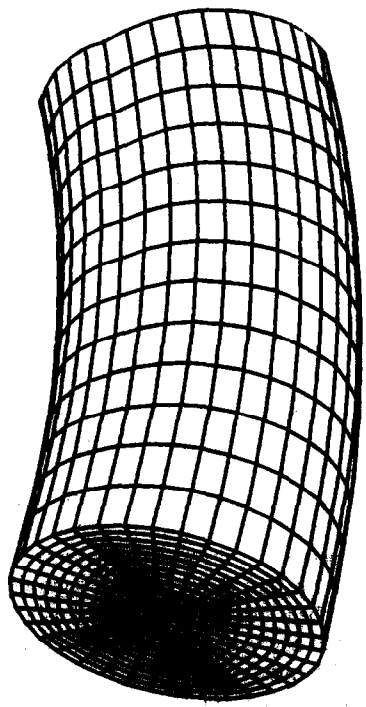

Fig. 2. Unstructured grid of the helical pipe.

$$a_P\phi_P = \sum_{nb} a_{nb}\phi_{nb} + c_{sb} \tag{13}$$

where a_P represents the center coefficient, a_{nb} denotes the influence coefficient for the neighbor, and c_{sb} is the contribution of the constant part of the source term, S_c, in $S = S_c + S_p\phi$, and the boundary conditions. The SIMPLEC algorithm [21] was used to resolve the coupling between velocity and pressure. The algebraic equations were solved iteratively using an additive-correction multigrid method [22] with a Gauss–Seidel relaxation procedure. To accelerate convergence, the under-relaxation technique was applied to all dependent variables. In the present study, the under-relaxation factor for p is 0.3, that for T is 1.0, and that for u_i is 0.7. The numerical computation is considered to be converged when the residual summed over all the computational nodes at the nth iteration for variables ϕ, R_ϕ^n, satisfies the following criterion:

$$\frac{R_\phi^n}{R_\phi^m} \leqslant 10^{-5} \tag{14}$$

where ϕ applies for u_i and T, and R_ϕ^m denotes the maximum residual value after m iterations.

A grid refinement study was conducted to determine an adequate grid distribution for the investigated physical problem. It was found that within a domain of $0° \leqslant \varphi \leqslant 270°$, a nonuniform grid distribution (sectional × axial) of 500×160 can ensure a satisfactory solution for the fluid flow and heat transfer in helical pipes, where the sectional number refers to the total number of elements on one cross section (φ = constant) of the pipes. With a grid of 500×160 and even finer, the difference between the solutions for the fluid flow and heat transfer was in the order of approximately 1%. Therefore, the numerical results presented in this paper are based on a grid system of 500×160 per 270° of φ.

All the computations in this paper were carried out on a Sun Sparc20 workstation in the Hemispheric Center for Environmental Technology at Florida International University. Approximately 300–350 iterations were needed to obtain the convergence results.

RESULTS AND DISCUSSION

The following numerical results were based on the physical properties for water ($Pr = 7.02$). The fully developed friction factor, f_{fd}, and the fully developed Nusselt number, Nu_{fd}, are defined as the asymptotic values of developing f_θ and Nu_θ, respectively, when further variation of f_m and Nu_m with axial distance are no more than 1%.

Comparison with existing data (fully developed results)

Due to the limited data on laminar developing convection in helical pipes of finite pitch, especially subject to a constant wall temperature boundary condition, the present predictions were compared

mainly with those presented in previous studies on fluid flow and heat transfer in helical pipes with zero pitch under the same boundary conditions. A typical case for this comparison was at $Re = 1000$, and $\delta = 0.050$. It was found that the values predicted for f_{fd} and Nu_{fd} by means of the parabolic numerical method are usually lower than those predicted by the fully elliptic method.

Table 1 provides a comparison of the present prediction for the fully developed friction factor with experimental data [23, 24] and parabolic numerical results [25]. As can be observed, the present numerical result for f_{fd} agrees fairly well with the experimental measurements, especially with those reported by Mishra and Gupta [24]. The difference for f_{fd} between the present elliptic numerical result and the previous parabolic numerical result reported by Liu and Masliyah [25] is approximately 2%.

Table 2 presents a comparison of the present computation of the fully developed Nusselt number with previous experimental measurements [26] and theoretical studies [15, 27]. The correlation proposed by Manlapaz and Churchill [27] was based on a regression analysis of the data available before 1980. It can be observed that the present numerical result for Nu_{fd} is almost the same as that in the experimental data reported by Schmidt [26]. The deviation of the parabolic numerical result for Nu_{fd} reported by Liu and Masliyah [15] from the elliptic numerical data is about 12%. This deviation is much higher than that for f_{fd} (about 2%), indicating that the accuracy for Nu_{fd} resulting from parabolic computation is lower than it is for f_{fd}.

Development of flow fields

Typical developments of temperature, axial and secondary velocity fields are shown in Fig. 3. On a plane with a small φ, a weak secondary flow is induced owing to the effects of curvature, with one vortex core appearing near the top and the other near the bottom of the cross section. Fluid with uniform temperature and axial velocity occupies most of the area of the cross section (the main potential core). As φ increases, the displacement effect of the growing boundary layer accelerates the flow in the main core, and the intensity of secondary flow increases. The unbalanced centrifugal force of the main flow results in a shift of the points of maximum velocity and temperature to the outside of the pipe. When φ is large enough, e.g. $\varphi = 270°$, as shown in Fig. 3(d), fluid with higher

Table 1. Comparison of the fully developed friction factor with previous studies

Previous study	Comments	Deviation from present elliptic numerical study [%]
Srinivasan *et al.* [23]	Experimental study $f_{fd} = 0.419De^{0.275}$ $De = Re\,\delta^{1/2}$	9.4
Mishra and Gupta [24]	Experimental study $f_{fd}/f_s = 1+0.0033\ (\log Dn_m)^4$ $f_s = 16/Re$ $Dn_m = Re[1/\delta(1+\lambda^2)]^{-0.5}$	2.03
Liu and Masliyah [25]	Parabolic numerical study $f_{fd}\,Re = [16+(0.378Dn\,\lambda_R^{1/4}+12.1)Dn^{1/2}\,\lambda_R^{1/2}\gamma^2$ $\{1+[(0.0908+0.0233\lambda_R^{1/2})\mathrm{Dn}^{1/2}$ $0.132\lambda_R^{1/2}+0.37\lambda_R 0.2]/[1+49/\mathrm{Dn}]\}$ $\lambda_R = \mathrm{R_c}/[\mathrm{R_c^2}+(\mathrm{H}/2\pi)^2]$ $\eta_R = (H/2\pi)/[R_c^2+(H/2\pi)^2]$ $Dn = Re\,\lambda_R^{1/2},\ \lambda = \eta_R/(\lambda_R\,Dn)^{1/2}$	2.08

Table 2. Comparison of fully developed Nusselt number with previous studies

Previous study	Comments	Deviation from present elliptic numerical study [%]
Schmidt [26]	Experimental study $Nu_{fd} = 3.65+0.08[1+0.8\delta^{0.9}]Pr^{1/3}\,Re^m$ $m = 0.5+0.2903\delta^{0.194}$	0.10
Manlapaz and Churchill [27]	Analysis of available data $Nu_{fd} = [(3.657+4.343/C_1)^3+1.158(De/C_2)^{3/2}]^{1/3}$ $C_1 = (1.0+957De^{-2}/Pr)^2$ $C_2 = 1.0+0.477/Pr$	16.5
Liu and Masliyah [15]	Parabolic numerical study $Nu_{fd} = 3.657+[(0.75Dn^{1/2}+0.0028Pr)Pr^{1/8}]/$ $[(1.0+0.00174Pr^{-3})(1.0+70.6Pr^{-0.6}/Dn)]$	12.1

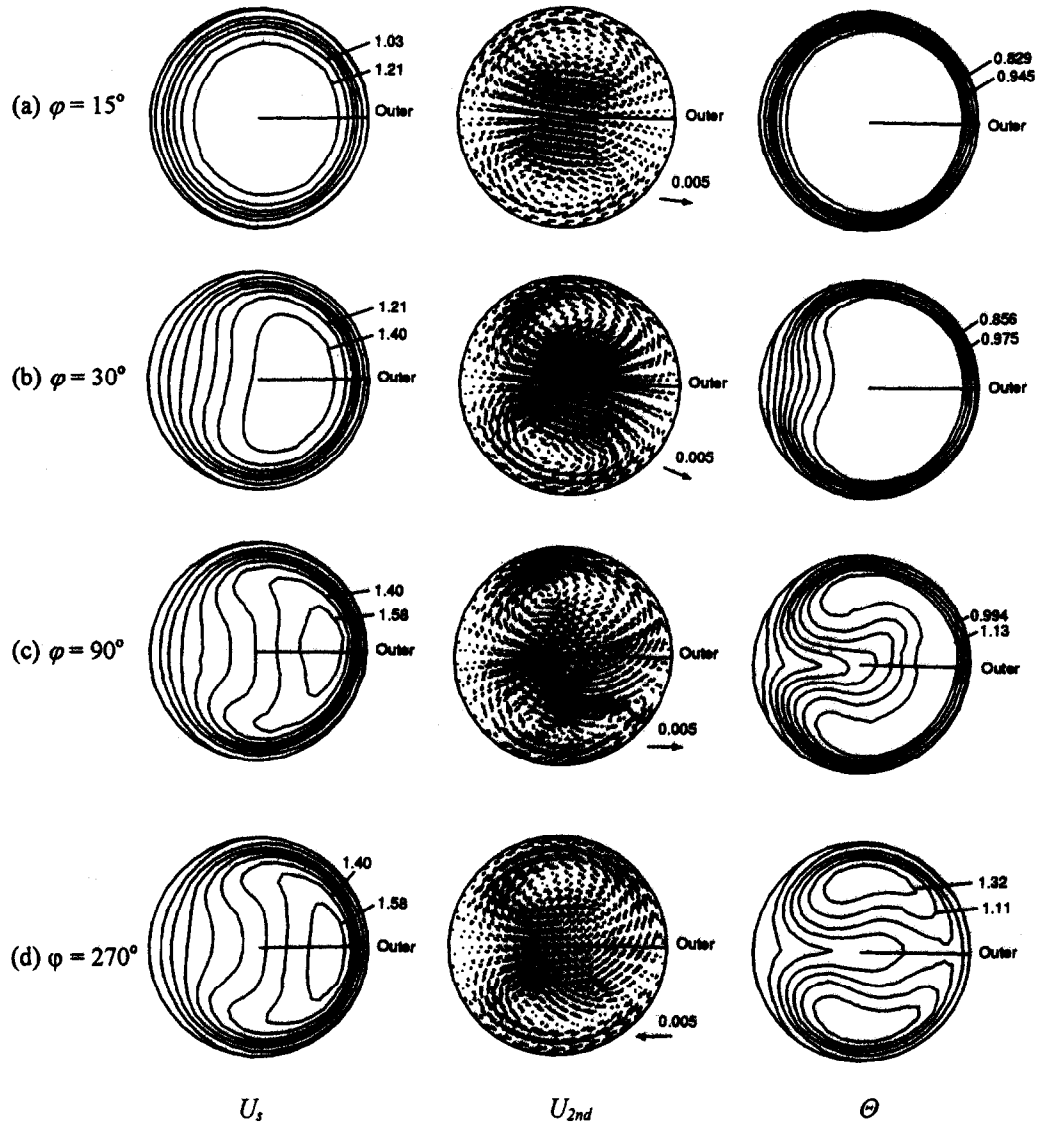

Fig. 3. Developments of velocity and temperature fields. $Re = 1000$, $\delta = 0.05$, $\lambda = 0.6$.

temperature is circulated within the two vortex zones of the secondary flow, with the region between the two zones being of relatively lower temperature.

As the laminar flow develops downstream from the inlet, the secondary flow always possesses two vortices over the entire developing region. As is well known, the flow fields are symmetric to the centerline connecting the outermost and innermost points of the cross section when $\lambda = 0.0$. For the case of Fig. 3, where $\lambda \neq 0$, the torsion caused by the finite pitch results in asymmetric developing flow fields. The zones of higher values of U_s and Θ are rotated clockwisely toward the bottom of the cross section, and the top secondary flow vortex is enlarged, especially when the value of φ is large.

Development of local friction factor and Nusselt number

Figure 4 shows the development of the local friction factors and Nusselt numbers with the increase of φ on the circumference of the helical pipe. The data are plotted in the direction from bottom ($r/a = -1.0$) to top ($r/a = 1.0$) of the pipe cross section. For a cross section at the given φ, the higher and lower values of f_θ (or Nu_θ) at $r/a = 0.0$ correspond to the friction factors (or Nusselt numbers) at the outermost and innermost points of the pipe, respectively. Generally speaking, in the region near the inlet, the distribution of f_θ (or Nu_θ) on the circumference is relatively smooth. As the flow proceeds downstream, the magnitude difference of f_θ (or Nu_θ) between the outer and inner sides of the pipe increases. When $\varphi = 15$, 30, 90 and 270°, the maximum difference ratio of the local friction factor on a cross section, $(f_{\theta,\max} - f_{\theta,\min})/f_m \times 100\%$, is 41.2, 80.3, 104.8 and 121.5%, respectively; and the maximum difference ratio of the local Nusselt number on a cross section, $(Nu_{\theta,\max} - Nu_{\theta,\min})/Nu_m \times 100\%$, is 67.9, 128.5, 165.5 and 143.3%, respectively.

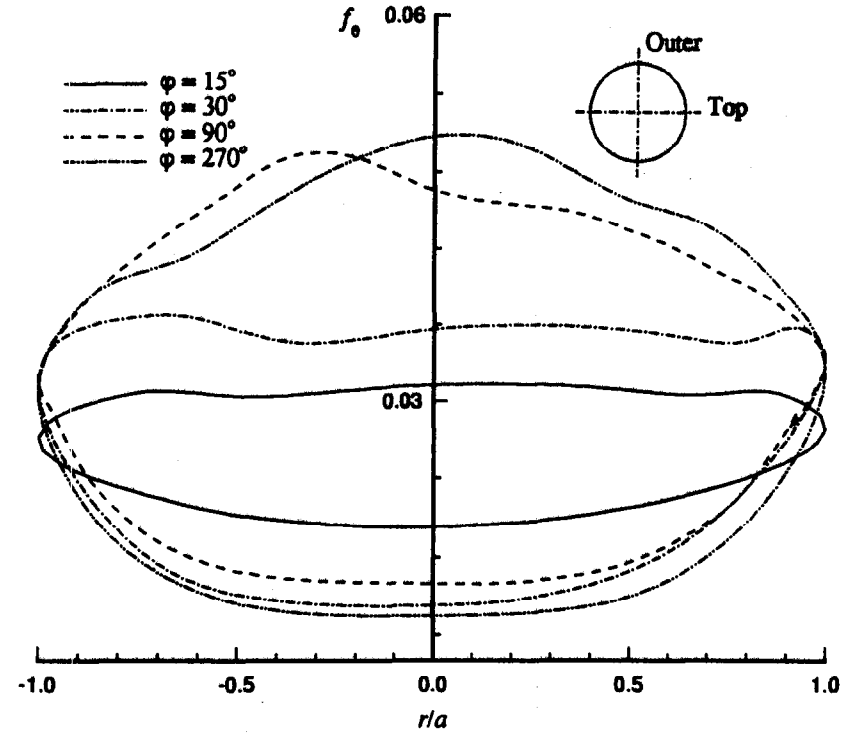

(a)

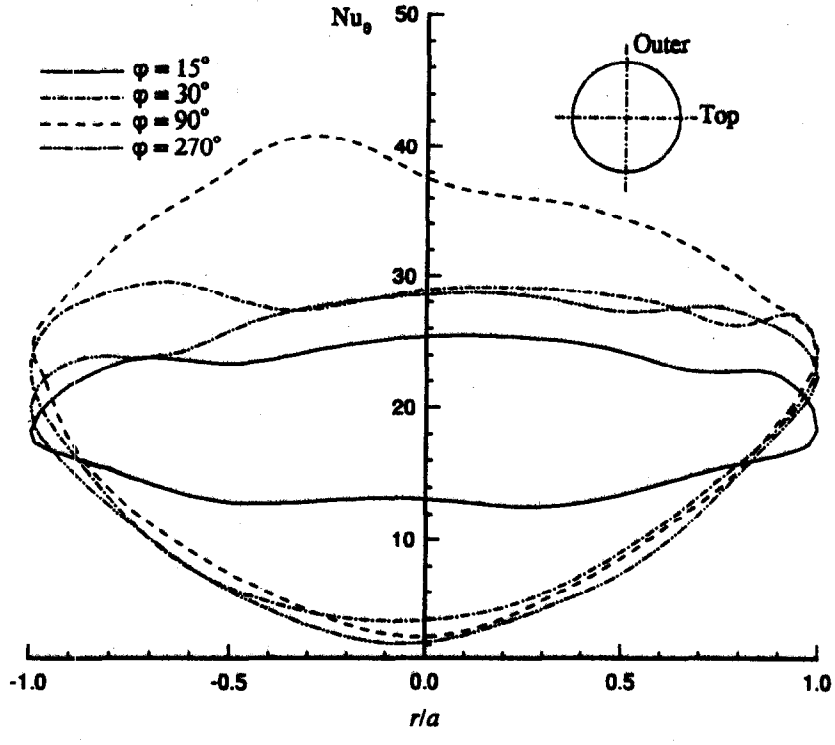

(b)

Fig. 4. Development of local friction factor (a) and local Nusselt number (b) on the circumference of a helical pipe. $Re = 1000$, $\delta = 0.05$, $\lambda = 0.6$.

If $\lambda = 0$, the distribution of f_θ (or Nu_θ) at each φ should be symmetric to the center line ($r/a = 0.0$) connecting the innermost and outermost points of the pipe. When $\lambda \neq 0$ (Fig. 4, $\lambda = 0.6$), the distribution of f_θ (or Nu_θ) is asymmetric to the center line due to the effect of the finite pitch, especially in the later stages of flow development. Interestingly, the effect of pitch on the distribution of f_θ (or Nu_θ) is more severe on the outer side than that on the inside of the helical pipe. The location of the maximum value of f_θ (or Nu_θ) has been found to shift as the flow proceeds downstream.

Development of average friction factor and Nusselt number

Effects of pitch. The development of the circumferential average friction factor and Nusselt number with axial location at different pitches is depicted in Fig. 5. The whole process of the development of f_m (or Nu_m) can be divided into three stages characterized by a substantially different nature. These are summarized below.

(1) The early developing stage ($\varphi < 15°$), in which f_m (or Nu_m) drops sharply as φ increases due to the rapid development of the flow (or thermal) boundary layer.
(2) The oscillatory developing stage ($15° < \varphi < 180°$), in which obvious oscillation of f_m (or Nu_m) appears with the increase of φ.
(3) The late developing stage ($\varphi > 180°$), in which f_m (or Nu_m) varies smoothly with φ until the fully developed flow (or heat transfer) is established.

It was ascertained that the oscillation of f_m (or Nu_m) is a consequence of the secondary flow. A similar oscillatory development of the Nusselt number was also found by Liu and Masliyah [15] and Patankar *et al.* [8] in their parabolic numerical studies of the laminar developing heat transfer in helical pipes.

Under the computational conditions used in Fig. 5, two peak values of Nu_m emerge after the early developing stage. The number of peak values of f_m appearing after the early developing stage depends on the value of λ. When the value of λ is larger than 0.2, the number of peak values of f_m is three. Within any stage, the effect of pitch is to reduce the magnitude of Nu_m. Within the early and late developing stages, the effect of pitch is to reduce the magnitudes of f_m. Within the oscillatory stage, the magnitude of f_m at higher λ may exceed that at lower λ, depending upon the axial location.

Effects of curvature ratio. Figure 6 demonstrates the effect of the curvature ratio, δ, on the development of f_m and Nu_m under given Re and λ. The curvature ratio exerts a similar influence on the developing f_m as it does on the developing Nu_m. In the course of flow and heat transfer development of the helical pipe, the effect of δ is to increase the magnitudes of f_m and Nu_m at different axial locations. Within the examined parameter ranges, both the amplitude and frequency of the oscillation of f_m and Nu_m are reduced with the increase of δ. Within the region close to the inlet, the laminar flow at higher δ needs a larger axial angle to reach the minimum values of f_m and Nu_m. With the increase of δ, the axial location of the maximum values of f_m and Nu_m within the oscillatory stage move downstream.

Effects of Reynolds number. The effects of the Reynolds number, Re, on the development of f_m and Nu_m are shown in Fig. 7 for the given δ and λ. When Re increases, the magnitude of f_m at every axial location of the pipe decreases; in contrast, the magnitude of Nu_m at every axial location of the pipe increases. With increasing Re, the oscillation of f_m diminishes, but the oscillation of Nu_m strengthens. Within the region close to the inlet, the axial angle required for the laminar flow to reach the minimum value of f_m or Nu_m is weakly affected by the variation of Re. Within the oscillatory stage, the axial location of maximum Nu_m moves downstream with the increase of Re. Re has a very weak effect on the axial location of maximum values of f_m in the oscillatory stage.

CONCLUSIONS

Three-dimensional developing laminar fluid flow and heat transfer in helical pipes with finite pitch have been simulated with a CVFEM. The fully elliptic numerical predictions in this study are quite consistent with existing experimental data. It has been found that a parabolic numerical method for this kind of problem results in a higher deviation in the Nusselt number than that in the friction factor.

Throughout the process of flow development, the laminar flow inside the helical pipes maintains a two-vortex-type asymmetric secondary flow pattern. As the laminar flow develops downstream, the non-uniformity of the temperature field increases until two zones of higher temperature cover the two zones of recirculating secondary flow.

The development of local friction factor or Nusselt number on the inner and outer sides of the helical pipes has been found to be different. As the flow proceeds downstream, the location of the maximum value of the local friction factor or local Nusselt number shifts on the circumference of the helical pipe.

As the flow proceeds downstream, both the average friction factor and the average Nusselt number are found to be oscillatory before the flow and heat transfer are fully developed. The effect of pitch is to reduce the magnitude of both the average friction factor and the average Nusselt number at different axial locations, except for the average friction factor in the oscillatory stage when the value of pitch is sufficiently high.

The effect of curvature ratio on the development of average friction factor is similar to its effect on the average Nusselt number. When the curvature ratio decreases, the oscillations of both the friction factor and the Nusselt number are enhanced.

Laminar flow at a higher Reynolds number generates a weaker oscillation of the average friction fac-

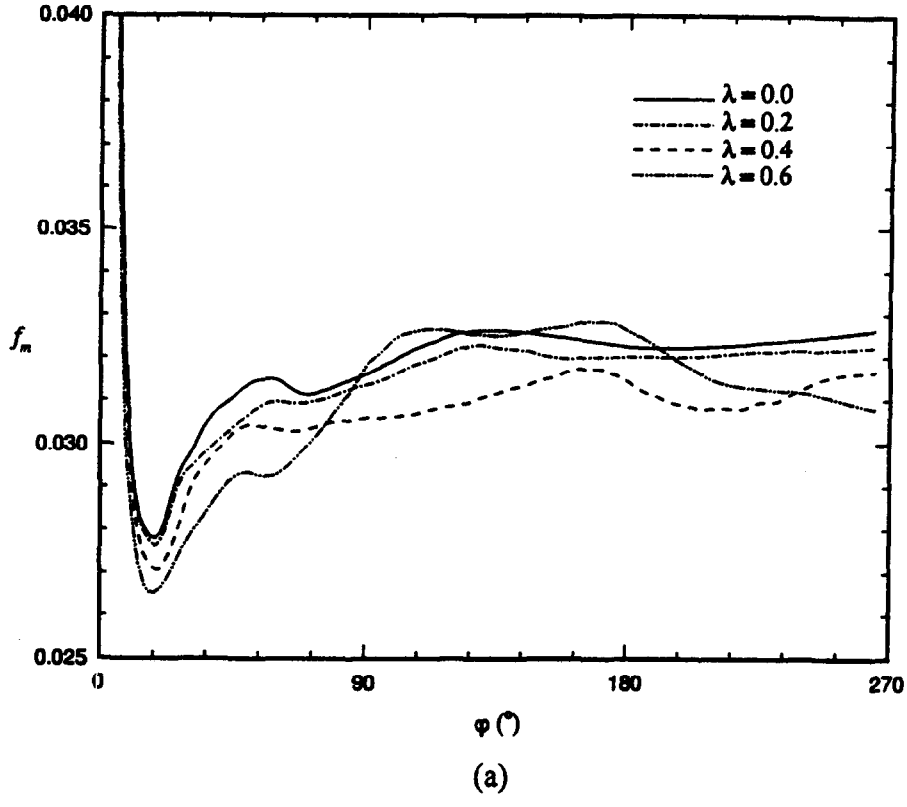

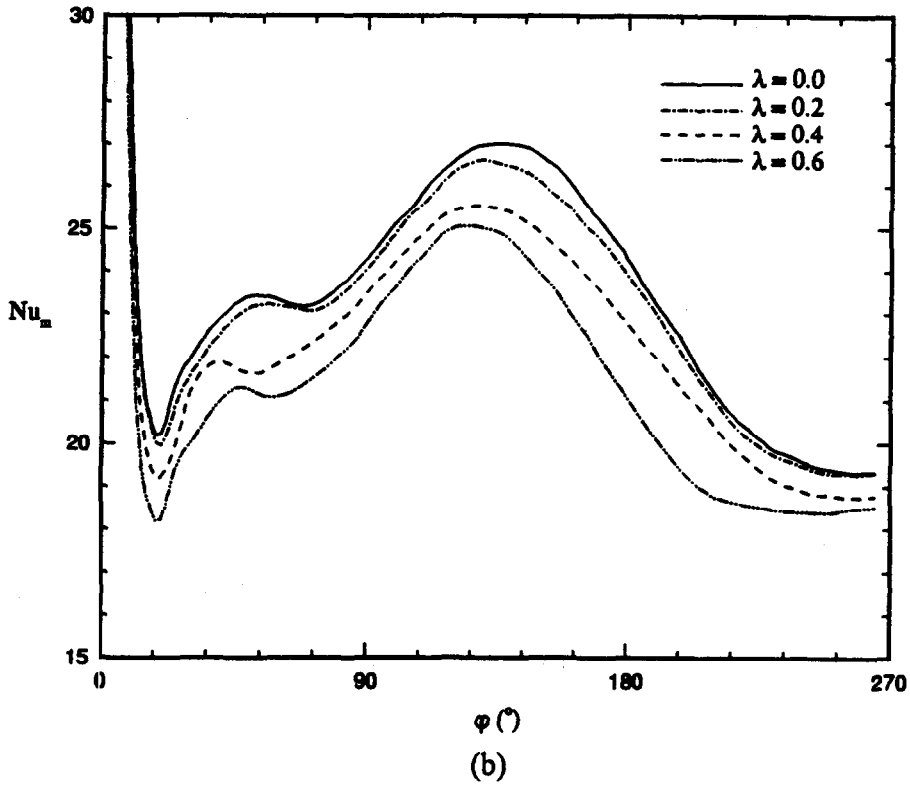

Fig. 5. Effects of pitch on the development of average friction factor (a) and average Nusselt number (b) on the circumference of a helical pipe. $Re = 1000$, $\delta = 0.05$.

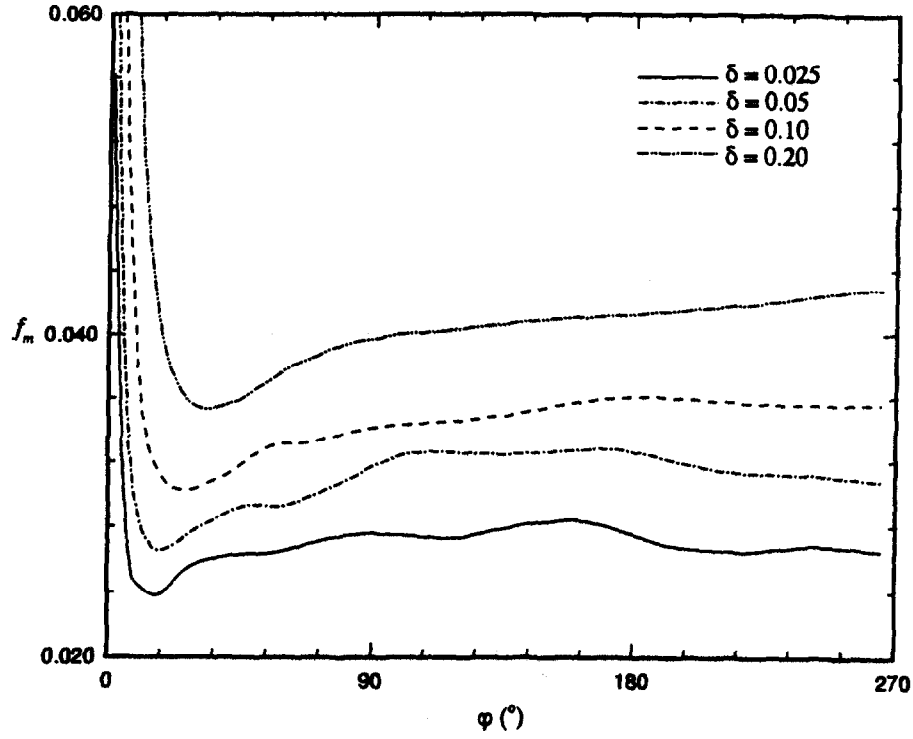

(a)

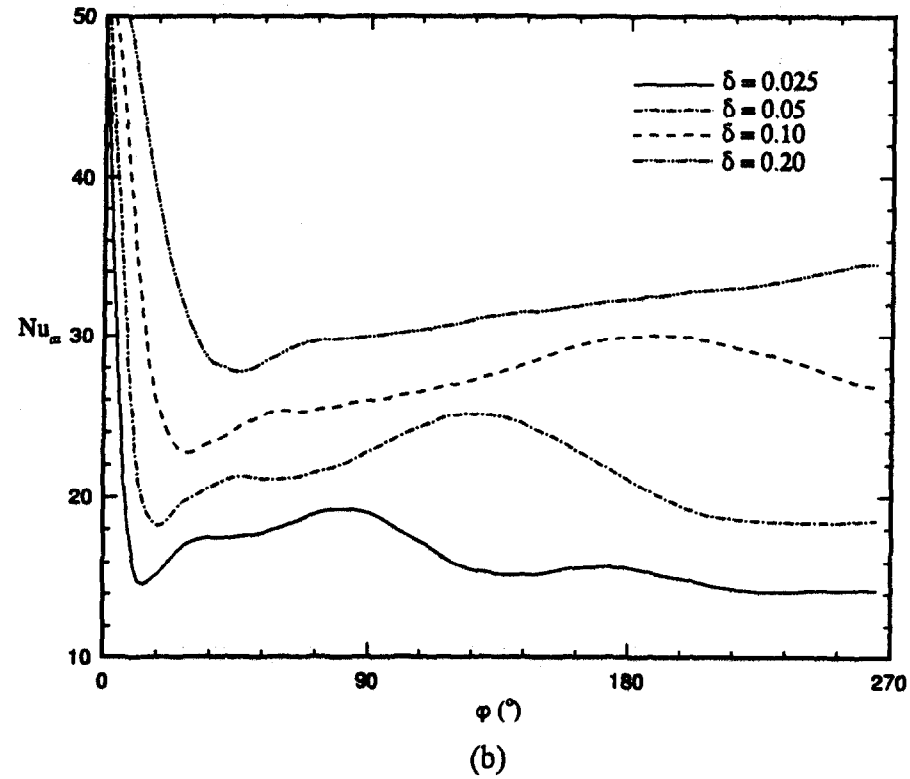

(b)

Fig. 6. Effects of curvature ratio on the development of average friction factor (a) and average Nusselt number (b) on the circumference of a helical pipe. $Re = 1000$, $\lambda = 0.60$.

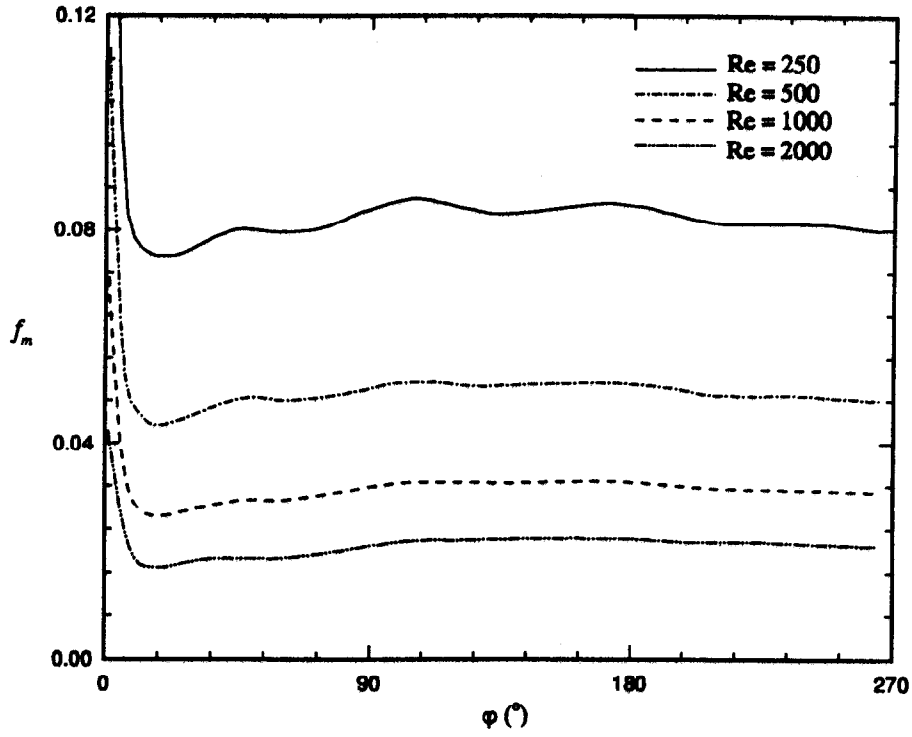

(a)

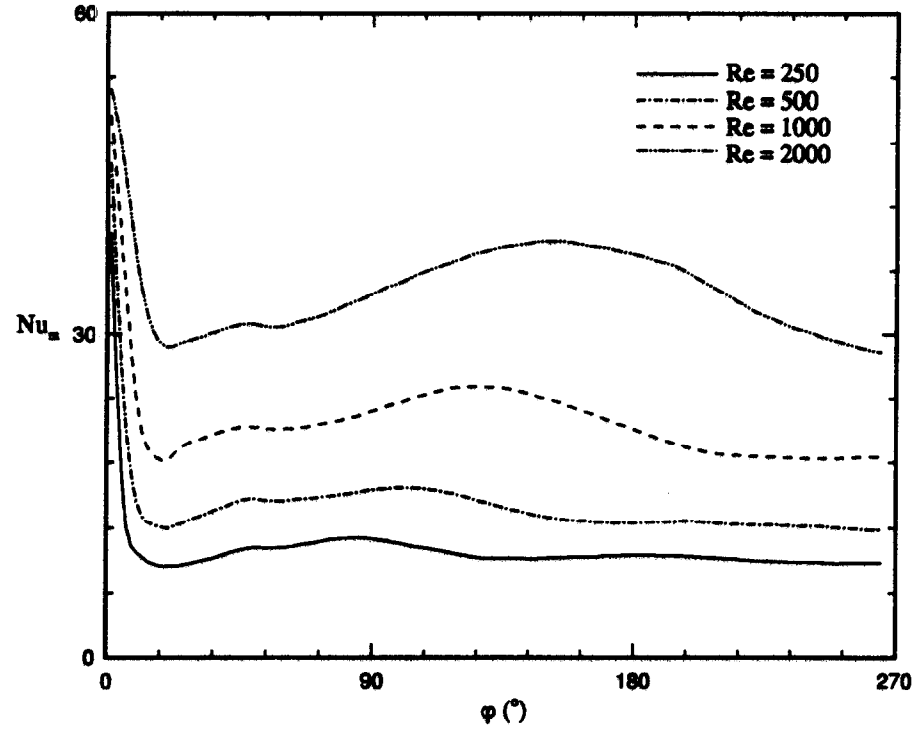

(b)

Fig. 7. Effects of Reynolds number on the development of average friction factor (a) and average Nusselt number (b) on the circumference of a helical pipe. $\delta = 0.05$, $\lambda = 0.60$.

tor than that at a lower Reynolds number. With the increase of the Reynolds number, the amplitude of the oscillation of average Nusselt number increases.

Acknowledgement—The authors gratefully acknowledge the financial support of the National Science Foundation (NSF) under Grant no. CTS-9017732.

REFERENCES

1. Berger, S. A., Talbot, L. and Yao, L. S., Flow in curved pipes. *Annual Review of Fluid Mechanics*, 1983, **15,** 461–512.
2. Shah, R. K. and Joshi, S. D., Convective heat transfer in curved ducts. In *Handbook of Single-phase Convective Heat Transfer*, eds S. Kakac, R. K. Shah and W. Aung. John Wiley, New York, 1987, Chap. 5.
3. Dravid, A. N., Smith, K. A., Merrill, E. W. and Brian, P. L. T., Effect of secondary fluid motion on laminar flow heat transfer in helically coiled tubes. *A.I.Ch.E. Journal*, 1971, **17,** 1114–1122.
4. Balejova, M., Cakrt, J. and Mik, V., Heat transfer for laminar flow in curved pipes with uniform wall heat flux. *Acta Technica Csav*, 1977, **22,** 183–194.
5. Janssen, L. A. and Hoogendoorn, C. J., Laminar convective heat transfer in helical coiled tubes. *International Journal of Heat and Mass Transfer*, 1978, **21,** 1197–1206.
6. Kalb, C. E. and Seader, J. D., Entrance region heat transfer in a uniform wall-temperature helical coil with transition from turbulent to laminar flow. *International Journal of Heat and Mass Transfer*, 1983, **26,** 23–32.
7. Austen, D. S. and Soliman, H. M., Laminar flow and heat transfer in helically coiled tubes with substantial pitch. *Experimental Thermal and Fluid Science*, 1988, **1,** 183–194.
8. Patankar, S. V., Pratap, V. S. and Spalding, D. B., Prediction of laminar flow and heat transfer in helically coiled pipes. *Journal of Fluid Mechanics*, 1974, **62**(3), 539–551.
9. Tarbell, J. M. and Samuels, M. R., Momentum and heat transfer in helical coils. *Chemical Engineering Journal*, 1973, **5,** 117–127.
10. Akiyama, M. and Cheng, K. C., Laminar forced convection in the thermal entrance region of curved pipes with uniform wall temperature. *Canadian Journal of Chemical Engineering*, 1974, **52,** 234–240.
11. Soh, W. Y. and Berger, S. A., Laminar entrance flow in a curved pipe. *Journal of Fluid Mechanics*, 1984, **148,** 109–135.
12. Padmanabhan, N., Entry flow in heated curved pipes. *International Journal of Heat and Mass Transfer*, 1987, **30,** 1453–1463.
13. Acharya, N., Sen, M. and Chang, H. C., Thermal entrance length and Nusselt numbers in coiled tubes. *International Journal of Heat and Mass Transfer*, 1994, **37,** 336–340.
14. Sillekens, J. J. M., Laminar mixed convection in ducts. Ph.D. thesis, Technische Universiteit Eindhoven, 1995.
15. Liu, S. and Masliyah, J. H., Developing convective heat transfer in helical pipes with finite pitch. *International Journal of Heat and Fluid Flow*, 1994, **15,** 66–74.
16. Germano, M., On the effect of the torsion in a helical pipe flow. *Journal of Fluid Mechanics*, 1982, **125,** 1–8.
17. Austin, L. R. and Seader, J. D., Entry region for steady viscous flow in coiled circular pipes. *A.I.Ch.E. Journal*, 1974, **20,** 820–822.
18. Baliga, B. R. and Patankar, S. V., A control volume finite-element method for two-dimensional fluid flow and heat transfer. *Numerical Heat Transfer*, 1983, **6,** 245–261.
19. *FLUENT/UNS User's Guide*, release 4.0. Fluent, Lebanon, NH, 1996.
20. *Geomesh User's Guide*, release 3.0. Fluent, Lebanon, NH, 1996.
21. Van Doormaal, J. P. and Raithby, G. D., Enhancements of the SIMPLE Method for predicting incompressible flow problem. *Numerical Heat Transfer*, 1984, **7,** 147–158.
22. Hutchinson, B. R. and Raithby, G. D., A multigrid method based on the additive correction strategy. *Numerical Heat Transfer*, 1986, **9,** 511–537.
23. Srinivasan, P. S., Nandapurkar, S. S. and Holland, F. A., Friction factors for coils. *Transactions of the Institute of Chemical Engineers*, 1970, **48,** T156–T161.
24. Mishra, P. and Gupta, S. N., Momentum transfer in curved pipes: Newtonian fluids. *Industrial and Engineering Chemistry, Process Design and Development*, 1979, **18,** 130–137.
25. Liu, S. and Masliyah, J. H., Axially invariant laminar flow in helical pipes with a finite pitch. *Journal of Fluid Mechanics*, 1993, **251,** 315–353.
26. Schmidt, E. F., Wärmeübergang und druckverlust in rohrschlangen. *Chemie-Ingemieur-Technik*, 1967, **13,** 781–787.
27. Manlapaz, L. and Churchill, S. W., Fully developed laminar convection from a helical coil. *Chemical Engineering Communications*, 1981, **9,** 185–200.